STATE OF THE CLIMATE IN 2014

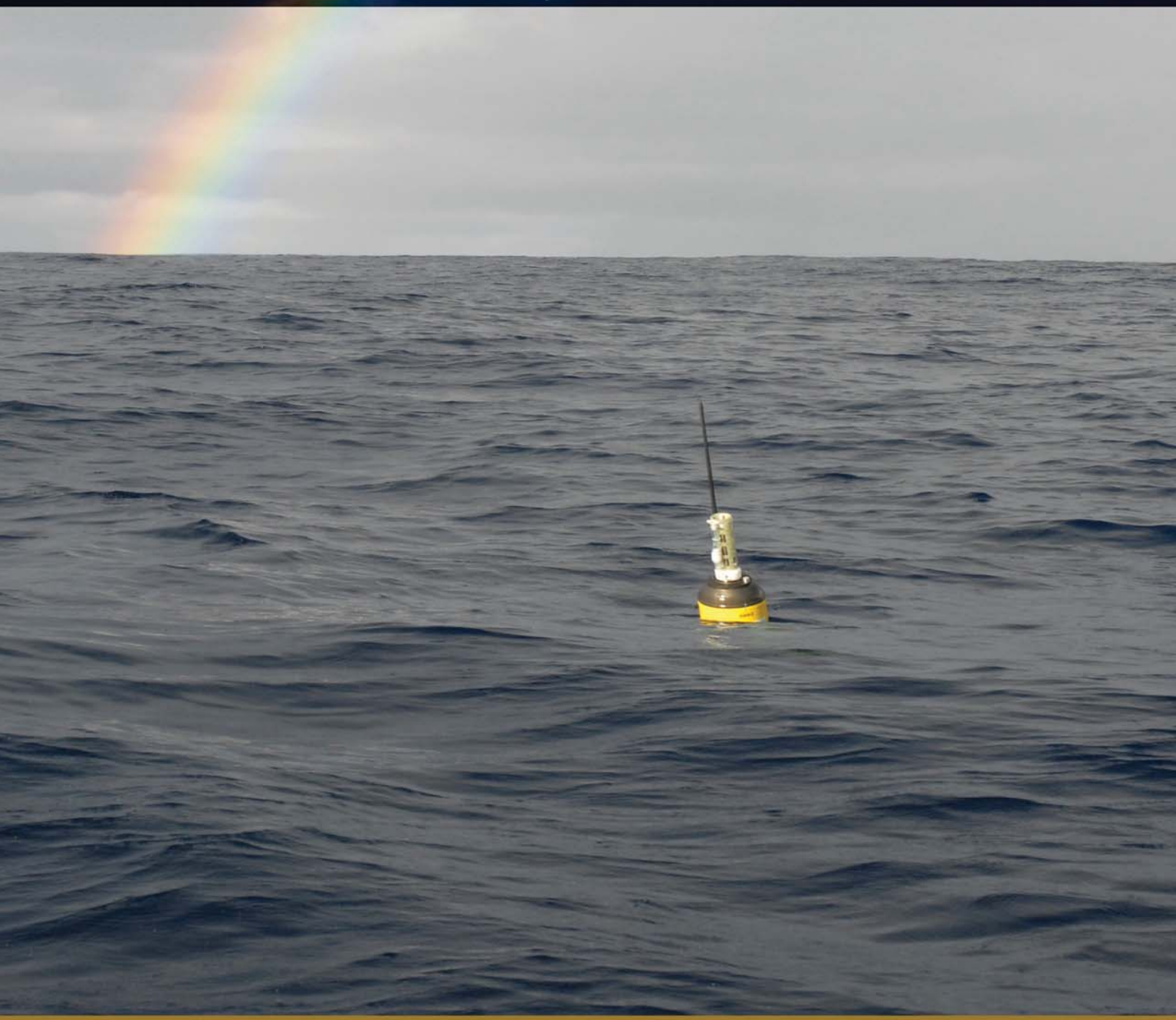

Special Supplement to the
Bulletin of the American Meteorological Society
Vol. 96, No. 7, July 2015

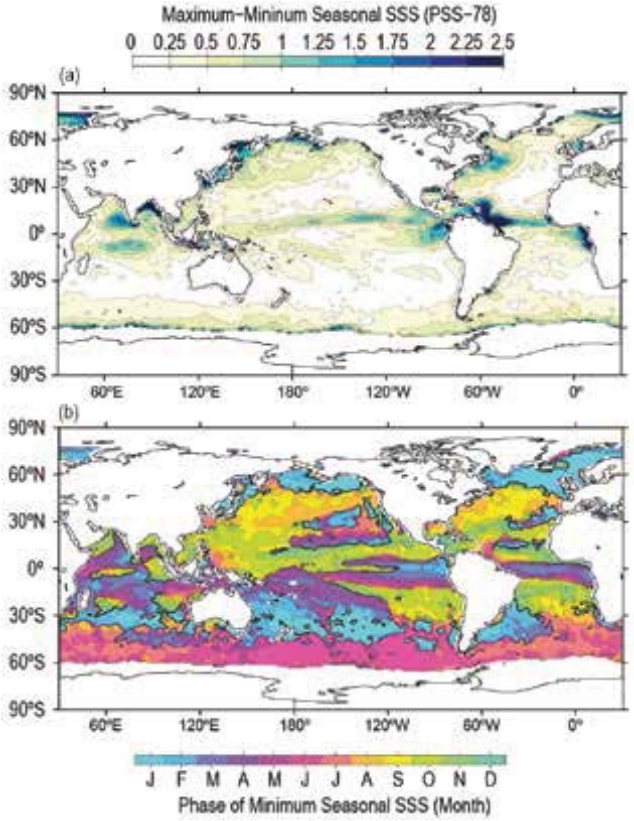

Fig. 3.13. (a) Values of seasonal maximum SSS minus seasonal minimum SSS from fits of annual and semi-annual harmonics at each location to 40 months (Sep 2011–Dec 2014) of detrended, gridded, smoothed *Aquarius* V3 monthly maps of SSS (colors in PSS-78), and (b) month of the minimum SSS estimate from those harmonics (colors). White ocean areas have excessive land or ice contamination in the *Aquarius* field of view.

minimum SSS in January–March, also at the end of summer. SSS at higher latitudes reaches a minimum in winter of both hemispheres.

f. Subsurface salinity—T. Boyer, J. Antonov, J. Reagan, C. Schmid, and R. Locarnini

Variations in subsurface salinity are important for constraining evaporation minus precipitation ($E–P$) estimates. Reanalysis products have significant differences in $E–P$ changes over the ocean (Trenberth et al. 2011). SSS fields are useful (Schmitt 2008; Yu 2011), but not sufficient alone to constrain $E–P$. Subsurface salinity information is vital since advection plays a role in moving ocean water that is altered by atmosphere–ocean interactions away from the atmosphere–ocean interface (Giglio and Roemmich 2014; Ren et al. 2014; Skliris et al. 2014). As surface-flux modified waters move to subsurface depths, surface changes are reflected in changes to ocean water mass composition and circulation patterns. Intensification of the water cycle reflected in increased SSS in areas dominated by evaporation and decreased SSS in areas dominated by precipitation over the last 50 years (Durack and Wijffels 2010; Durack et al. 2012; Skliris et al. 2014) has resulted in complex subsurface changes. Upper ocean salinity has increased globally in recent times compared to long-term means, while intermediate waters have decreased in salinity (Roemmich and Gilson 2009; Helm et al. 2010). Additionally, changes in salinity have an effect on sea level (Antonov et al. 2005; Durack et al. 2014).

To investigate interannual changes of subsurface salinity, all available subsurface salinity profile data for year 2014 were used to derive 1° mean gridded salinity anomalies from a long-term mean for years 1955–2006 (Antonov et al. 2010) at standard depths from the surface to 2000 m as described in Boyer et al. (2012). The single largest source at present of salinity profiles for the world's ocean is the Argo program with its fleet of profiling floats (Roemmich et al. 2009). A total of 146 723 profiles from 4456 floats from the Argo program were used in the process of calculating subsurface salinity anomalies for 2014. These data were primarily real-time with basic quality control, but many profiles include salinity drift adjustments that were based on delayed mode scientific quality control of earlier cycles in a float lifetime, and a small fraction of the profiles have undergone delayed mode scientific quality control. In addition to the Argo data, another major source of salinity data is 23 947 daily mean profiles from tropical moored buoys (www.pmel.noaa.gov/tao/) in all three oceans, usually limited to the upper 500 m. There were 13 168 conductivity–temperature–depth casts with salinity profiles for 2014, mainly obtained through the Global Temperature and Salinity Profile Project (GTSPP). Finally, 40 609 profiles from gliders were made available through GTSPP, the Australian Integrated Marine Observing System (IMOS), and the U.S. Integrated Ocean Observing System (IOOS).

Furthermore, in order to examine the year-to-year change in salinity, anomaly fields for 2013 were recalculated based on updated quality control provided by Argo. All salinity and salinity anomaly data were examined using quality control procedures outlined in Boyer et al. (2013) and are available through the World Ocean Database. All derived fields can be found at www.nodc.noaa.gov/OC5/3M_HEAT_CONTENT/.

Zonal mean differences between salinities in the Pacific Ocean in 2014 and the long-term mean (Fig. 3.14a) revealed that the South Pacific below 250 m was generally fresher in 2014 compared to the long-term mean, with the exception of the region south of

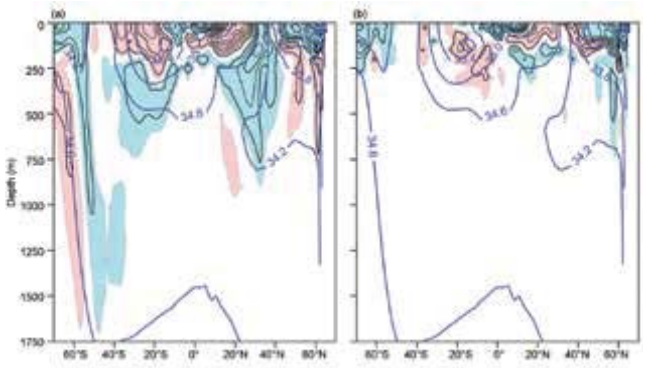

Fig. 3.14. Zonally averaged (a) 2014 salinity anomaly and (b) 2014 minus 2013 salinity for the Pacific Ocean. Blue shading represents negative (fresh) anomalies <–0.01, red shading represents positive (salty) anomalies >0.01. Anomalies are contoured at 0.02 intervals. Zonally averaged climatological mean salinity values (Antonov et al. 2010) are contoured (thick blue lines) at 0.4 intervals. All values are reported on the 1978 Practical Salinity Scale (PSS-78).

55°S where a deep salty anomaly reached from about 200-m to >1500-m depth. Upper ocean freshening relative to the long-term mean in this region deepened northward to 50°S, extending to a depth >1500 m, while near-surface waters were characterized by slightly higher salinities between 50°S and 45°S. Meijers et al. (2011) attributed freshening in this region to southward movement of the Antarctic Circumpolar Current and water mass changes possibly due to increased precipitation and ice melt. Above 250 m between 40°S and 15°S the Pacific was saltier than the long-term mean. Farther north, near 10°S, the salty anomaly was overlaid by an up to 150-m thick fresh anomaly. Conditions were saltier in 2014 than in 2013 in this area and extended northward to the equator at 200-m depth (Fig. 3.14b). Mean salinity in the upper 100 m (Fig. 3.11a) shows 2014 fresher than the long-term mean in the western equatorial Pacific, stretching east along bands roughly under the intertropical convergence zone (ITCZ) and South Pacific convergence zone (SPCZ). Conditions in this area were fresher in 2014 than 2013 (Fig. 3.11b) but saltier in the far western Pacific near Indonesia (Fig. 3.11b). While the ITCZ was an area of heavy precipitation, the lead mechanism for the low salinity zone near the ITCZ was wind-driven Ekman dynamics, and this feature was decoupled from the ITCZ in the Northern Hemisphere fall–winter (Yu 2014). Freshening from 2013 to 2014 in the area of the western Pacific warm pool was large enough to reverse the sign of the salinity anomaly relative to the long-term mean for 2014 from previous years (Boyer et al. 2014). In the North Pacific, salinity change >0.04 between 2013 and 2014 was limited to the upper 250 m south of 40°N. Salinity increases from 2013 to 2014 stretched from 5°N to 55°N; in the tropics and near 40°N this anomaly was submerged under a freshening layer. The northern area of freshening extended from 40°N to the Bering Strait and was mainly confined to the upper 200 m, with the exception of the northernmost region. Freshening was also seen near the Bering Strait from 2011 to 2012, while saltier conditions were found from 2010 to 2011 and from 2012 to 2013.

Between the mid-1950s and the mid-1990s an increase in salinity in the subtropical and tropical North Atlantic was coupled with a decrease in salinity in the subpolar North Atlantic (Curry et al. 2003; Boyer et al. 2007; Wang et al. 2010). Since the mid-1990s, both the subtropical and subpolar North Atlantic exhibit increased salinity (Boyer et al. 2007; Wang et al. 2010). This pattern changed in 2014 in the subpolar North Atlantic (Fig. 3.15a), with the freshening observed around 50°N expanding and deepening between 2013 and 2014 (Fig. 3.15b). This change may have been due to the commencement of deep water formation in the Labrador Sea in the winter of 2013/14 injecting fresh, cool water to depths >1700 m (Kieke and Yashayaev 2015; see Sidebar 3.2). Freshening below 50-m depth in the subtropical North Atlantic between 2012 and 2013 did not continue into 2014. Overall, there was little change from 2013 to 2014 in the subtropical North Atlantic, and most changes >0.02 were confined to the upper 250 m (Fig. 3.15b). Saltier conditions in the area south of 20°N in the North Atlantic reversed below 50 m while becoming saltier above 50 m near the equator.

In the Indian Ocean, differences between 2014 salinity zonal means and the long-term mean (Fig. 3.16a) included deep (>1000 m) freshening south of the equator, interrupted by increased salinity in the midlatitude south Indian Ocean from the surface to 800 m at 40°S that narrows at a depth of 250 m. In the upper 100 m (Fig. 3.11a), the fresh anomaly

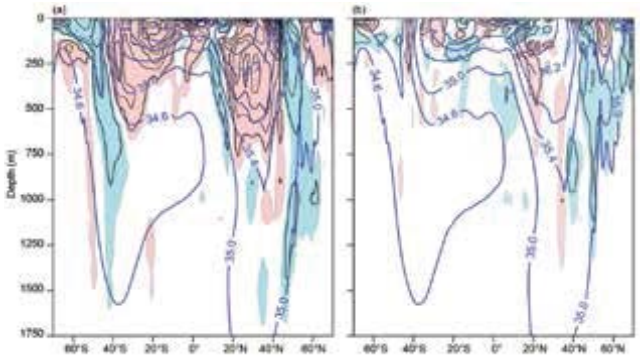

Fig. 3.15. Zonally averaged (a) 2014 salinity anomaly and (b) 2014 minus 2013 salinity field for the Atlantic Ocean. Details follow Fig. 3.14.

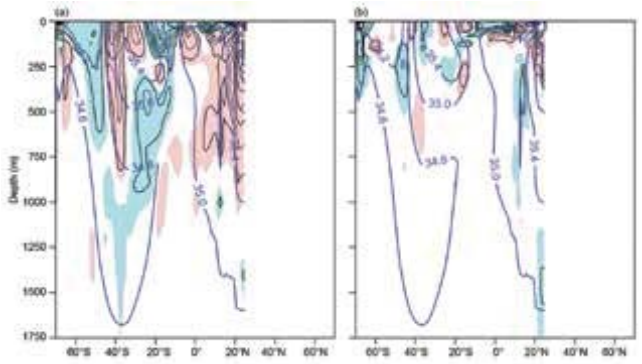

Fig. 3.16. Zonally averaged (a) 2014 salinity anomaly and (b) 2014 minus 2013 salinity field for the Indian Ocean. Details follow Fig. 3.14.

at latitudes north of 30°S covered most of the basin from Australia to Africa, a westward expansion that occurred over the last three years (Boyer et al. 2014). South of 30°S, the salty anomaly extended across the entire basin in a narrow band north of 50°S, a continuation of the pattern of 2013. The salinity change from 2013 to 2014 in the south Indian Ocean was small (<0.02; Fig. 3.16b), except south of 60°S where the data coverage is coarse, and in the upper 50 m near the equator. Most of the north Indian Ocean anomalies for 2014 continued to be salty to depths exceeding 700 m. From 2013 to 2014, changes in the north Indian Ocean were mainly confined to the upper 150 m, with a freshening in the upper 100 m within 5° of the equator and increasing salinity in the subtropics near the surface, which continued in the 50–150 m layer toward the equator.

g. Surface currents—K. Dohan, G. Goni, and R. Lumpkin

This section describes ocean surface current variability, emphasizing tropical events, western boundary currents, transports derived from ocean surface currents, and features such as rings (large eddies) inferred from surface currents. Global surface currents (Fig. 3.17) are obtained from satellite (sea surface height, wind stress, and SST) and in situ (global array of drogued drifters and moorings) observations and discussed by individual basin below. Current variability can also be derived from sources such as shipboard current measurements, expendable bathythermograph repeat sections, and underwater glider data. The strongest, most persistent anomaly in global surface currents in 2014 was the stronger-than-normal eastward flow of the Pacific North Equatorial Countercurrent (NECC). In addition, in the North Pacific, the Kuroshio and its extension remain about 1° north of their climatological positions in 2014.

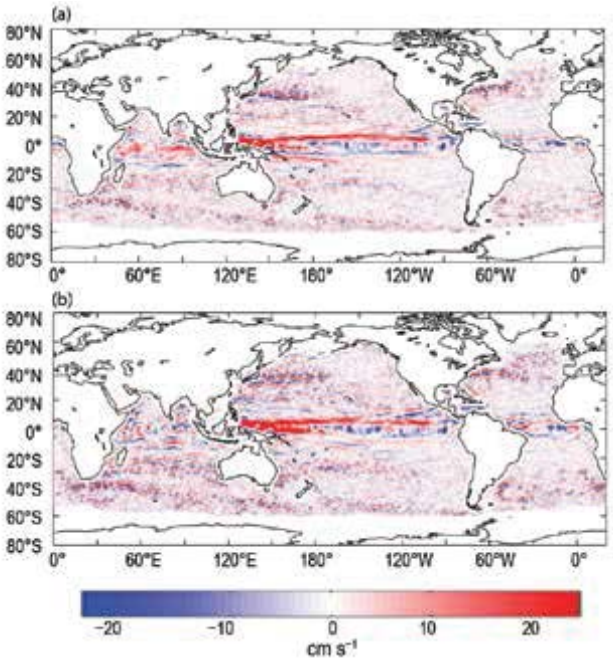

Fig. 3.17. Global zonal geostrophic surface current anomalies relative to 1993–2007 for (a) 2014 and (b) 2014–2013 (cm s^{-1}), based on OSCAR currents derived from altimetry, ocean vector winds, and SST (Bonjean and Lagerloef 2002; Dohan and Maximenko 2010).

1) Pacific Ocean

January 2014 began with a strengthening of climatological conditions. Westward anomalies of ~20 cm s^{-1} were present in the equatorial Pacific between 170° and 100°W. Farther east and north, between 160° and 120°W and at 7°N, eastward anomalies of ~20 cm s^{-1} indicated a strengthening of the NECC. This strengthening occurred throughout 2014 (Fig. 3.17), changing with the seasonal position, with monthly anomalies generally between 10 and 30 cm s^{-1}. February saw a dramatic change in equatorial currents. Eastward anomalies developed between 140°E and 150°W along the equator, ranging from 70 cm s^{-1} in the west to 40 cm s^{-1} in the east, and peaking above 1 m s^{-1} at 170°E. Westward anomalies of ~30 cm s^{-1} persisted along the equator east of 110°W. By March, eastward anomalies spanned the entire basin with some regions reaching over 1 m s^{-1}. These anomalies lessened some in April and May. June saw a complete reversal of the equatorial anomalies with strong westward anomalies present across the basin, ranging between 20 and 80 cm s^{-1}, strongest in the center of the basin, reaching a peak at 150°W. This continued through July, shifting to the east with anomalies of 50 cm s^{-1} between the dateline and 100°W, and then subsided in August. Some westward anomalies of ~10 cm s^{-1} were beginning to appear in December, west of 140°W.